# Energetic particle acceleration in a 3D magnetic field reconnection model: a role of MHD turbulence

T. Kobak* & M. Ostrowski

*Obserwatorium Astronomiczne, Uniwersytet Jagielloński, ul. Orla 171, 30-244 Kraków, Poland*
( *E-mail: kto@oa.uj.edu.pl)

**ABSTRACT**

The role of MHD turbulence in the cosmic ray acceleration process in a volume with a reconnecting magnetic field is studied by means of Monte Carlo simulations. We performed modelling of proton acceleration with the 3D analytic model of stationary reconnection of Craig et al. (1995) providing the unperturbed background conditions. Perturbations of particle trajectories due to a turbulent magnetic field component were simulated using small-amplitude pitch-angle momentum scattering, enabling modelling of both small and large amplitude turbulence in a wide wave vector range. Within the approach, no second-order Fermi acceleration process is allowed. Comparison of the acceleration process in models involving particle trajectory perturbations to the unperturbed one reveals that the turbulence can substantially increase the acceleration efficiency, enabling much higher final particle energies and flat particle spectra.

**Key words:** magnetic field: reconnection – cosmic rays – acceleration of particles - MHD – Sun: flares – turbulence

## 1 INTRODUCTION

Particle acceleration processes in regions of magnetic field reconnection can play an important role in various astrophysical sites by providing high energy particles, heating thermal plasma and by changing the magnetic field configuration (e.g. Somov 1994). The first of these processes, accelerating particles to cosmic ray energies, acts due to electric fields occurring in the reconnection region. Two approaches were applied to describe the acceleration process. In the more basic one, analytic or semi-analytic models for the reconnection region provided background for the derivation of particle trajectories and discussion of the energy distribution of particles escaping from the reconnection volume. A simple discussion of particle trajectories presented by Speiser (1965; see also Sonnerup 1971) shows that even a tiny magnetic field component near the neutral current sheet efficiently removes ergetic particles and decreases its final energy. Further studies by Stern (1979) and Wagner et al. (1981) revealed the importance of the O-type neutral line regions for the acceleration, due to partial particle trapping in the accelerating volume. Deeg et al. (1991) and Somov & Kosugi (1997) discussed several features of the acceleration process in the X-type stationary reconnection. The time dependent effects of the acceleration process were introduced by considering the background magnetic and electric fields as derived from simple MHD simulations (cf. Sato et al.

1982, Scholer & Jamitzky 1987, Atkinson et al. 1989, Zelenyi et al. 1990).

Substantial progress in considering realistic reconnection processes came from the two dimensional ($\equiv$ 2D; Matthaeus et al. 1984, Ambrosiano et al. 1988, Scholer & Jamitzky 1989, Veltri at al. 1998) and 3D (Birn & Hesse 1994, Schopper et al. 1999, Kliem et al. 1998) MHD modelling involving a perturbed magnetic field as the initial condition. This approach yields a complex structure with X-type and O-type null points and magnetic field perturbations of scales comparable to the macroscopic structure dimensions. Ambrosiano et al. (1988) show that such a turbulent neutral point mechanism influences the acceleration process in two ways. It enhances the reconnection magnetic field while producing a stochastic electric field that gives rise to momentum diffusion, and it also produces magnetic bubbles and other irregularities that can temporarily trap test particles in the strong reconnection field for times comparable to the magnetofluid characteristic time. As a result, the very flat particle spectra formed can extend to higher energies in comparison to the unperturbed conditions.

One should also note that a realistic description of the acceleration process requires considering the full 3D configuration of the reconnection region (e.g. Birn & Hesse 1994, Schopper et al. 1999, Veltri et al. 1998). Besides the role which the mean field structure plays, particle transport depends in a qualitative way on the turbulence dimensionality (cf. Giacalone & Jokipii 1994, Michałek & Ostrowski 1996)

and the involved wave modes (e.g. Schlickeiser & Miller 1997, Michałek & Ostrowski 1998).

Besides providing a substantial improvement in understanding of the process, a general deficiency of the above mentioned papers discussing particle acceleration in the turbulent reconnection regions are the complicated interrelations between such factors as the assumed or derived mean magnetic field structure, its dimensionality, the assumed or derived form of turbulence, and the particle acceleration process. For example in the paper of Ambrosiano et al. (1988) it was difficult to separate the role of diffusive particle motions from trapping by the structures formed in/near the reconnection layer. In order to clarify the situation, with only one of these factors modifying the acceleration process in turbulent reconnection, we decided to use a simple model which allows us to consider the role of random particle trajectory perturbations separately. The process acting in the vicinity of the X-type reconnection does not provide a means for particle trapping in the mean (unperturbed) structure of the reconnecting field. As described in the next section, we use the 3D analytic model of stationary reconnection of Craig et al. (1995) to define the background model, being a reference for the model involving particle pitch-angle momentum scattering due to MHD turbulence. Perturbations of particle trajectories due to a turbulent magnetic field component were simulated using small-amplitude pitch-angle momentum scattering, enabling modelling of both small and large amplitude turbulence in a wide wave vector range. No second-order Fermi acceleration processes are allowed within this approach. In section 3 we present results of particle energy spectrum modelling for different scattering amplitudes. Comparison of the acceleration process to the unperturbed one confirms that the turbulence can substantially increase the acceleration efficiency, enabling particles to form flat high-energy spectra with much increased final energies. Then, in section 4, we briefly summarize these results.

In the present simulations we scale the parameters of the reconnection region to those characteristic for the solar flare (e.g. Miller et al. 1997). However, we do not aspire to present a flare acceleration model. We provide all numerical values in SI units.

## 2   SIMULATIONS OF THE ACCELERATION PROCESS

### 2.1   The 3D reconnecting magnetic field structure

The considered reconnection region (Fig. 1) involves inflowing plasma from the 'top' and the 'bottom' toward the $x = 0$ plane, and outflowing to the sides. All physical quantities, the flow velocity, the magnetic field and the electric field are symmetric with respect to the *origin* of the reference frame, with the reconnection "plane" (magnetic field is strictly 0 only in a single point in the center) being slightly inclined with respect to the $x = 0$ plane. To describe this structure analytically we use a 3D model of the stationary reconnection by Craig et al. (1995), which provides the analytic structure for the magnetic field $\vec{B}$, the electric field $\vec{E}$ and the plasma velocity $\vec{V}$. The following parameters are introduced in this model: $\alpha$, $\lambda$, $\eta$ and $k$ define topologic structure of the magnetic field; $\mu$ define the reconnection
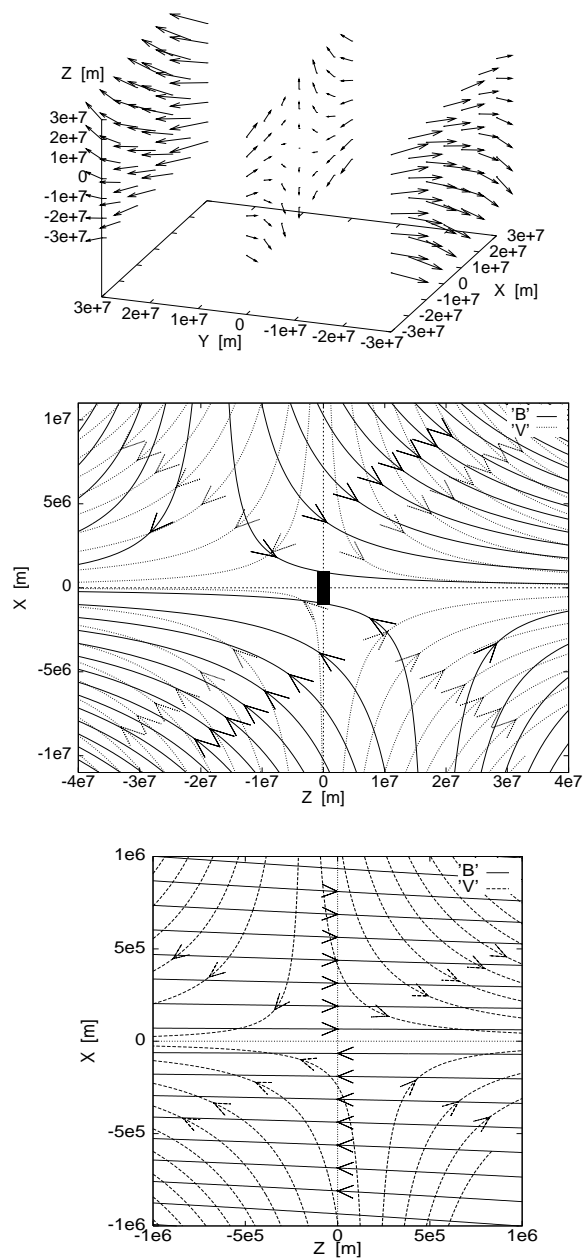


**Figure 1.** Upper panel: Magnetic field vectors in three layers $y = -3e7$, $y = 0$, $y = 3e7$ of the considered recconection volume. The y component of magnetic field vector has been increased 6 times to demonstrate of the stucture. Middle and bottom panels: The magnetic field structure (full lines) and the velocity field (dashed lines) in the $y = 0$ plane of the considered reconnection region. In both these panels the border of the figure also represents the particle escape boundary. One should note different scales along the axes in these panels. The small black rectangle in the middle shows the size of the region where particle scattering due to turbulence is imposed. In the lower panel, the structure of the unperturbed magnetic field and the velocity field in this small turbulent volume is presented.

area thickness; $\rho$ is the plasma density; $\xi$ denotes the external electric field component; $\mu_0$ is the magnetic permeability of the vacuum. With the use of these parameters and the notation involving a radius vector $\vec{r} = \{x\ ,\ y\ ,\ z\}$ and the unit vectors $\hat{x}$, $\hat{y}$ and $\hat{z}$ along the respective axes,

$$\vec{B} = \lambda \vec{P}(\vec{r}) + \vec{Q}(x) \qquad , \qquad (2.1)$$

$$\vec{V} = \left[ \vec{P}(\vec{r}) + \lambda \vec{Q}(x) \right] \frac{1}{\sqrt{\rho \mu_0}} \qquad , \qquad (2.2)$$

$$\vec{E} = \left[ -\frac{\sqrt{\pi}\eta}{2\mu_0} Z'(0) e^{-(\mu x)^2} \right] \hat{y} + \xi \left[ 1 - 2x\mu\, \mathrm{daw}(\mu x) \right] \hat{z} \qquad , \qquad (2.3)$$

where

$$\vec{P} = \alpha \left[ -x\hat{x} + ky\hat{y} + (1-k)z\hat{z} \right] \qquad , \qquad (2.4)$$

$$\vec{Q} = \frac{\xi}{\eta\mu} \sqrt{\frac{\mu_0}{\rho}} \mathrm{daw}(\mu x)\hat{y} + \left[ \frac{\sqrt{\pi}}{2\mu} Z'(0)\, \mathrm{erf}(\mu x) + Z(0) \right] \hat{z} \qquad , \qquad (2.5)$$

and

$$\mathrm{daw}(x) \equiv \int_0^x \exp(t^2 - x^2)dt \qquad , \qquad \mathrm{erf}(x) \equiv \int_0^x \exp(-t^2)dt \qquad ,$$

$$\mu^2 = \frac{\alpha}{2\eta} 1 - \lambda \quad .$$

The function $Z(x)$ of Craig et al. (1995) satisfies the differential equation

$$\alpha(1 - \lambda^2)[(1-k)Z + xZ'] + \eta Z'' = \alpha\gamma_2\lambda(2-k)x \quad , \quad (2.6)$$

where one requires $\gamma_2 k = 0$ ($\gamma_2$ or $k$ must be zero). With these expressions one can construct the reconnection region in two ways. It is possible to choose the parameters $\xi$, $Z'(0)$, $Z(0)$, $\alpha$, $\beta$, $\eta$, $\mu$ in such a way that either the magnetic field component $B_{\hat{z}}$ or $B_{\hat{y}}$ vanishes in some area:

- i.) $B_y$ vanishes where $\lambda\alpha ky = -\frac{\xi\mu_0}{\eta\mu} \mathrm{daw}(\mu x)$
- ii.) $B_z$ vanishes where $\beta(1-k)z = \frac{\sqrt{\pi}}{2\mu} Z'(0)\, \mathrm{erf}(\mu x)$.

The maximum value of $r$ allowing for one of the above conditions to be satisfied gives the half length of the reconnection region $L$ (a scale for the layer with negligible magnetic field near the null point). For example, for the case (ii) one has

$$L = \frac{\pi Z'(0)}{4\beta(1-k)\mu} \qquad . \qquad (2.7)$$

In the case (i), where the function $daw$ determines the behaviour of the magnetic field, the gradient of the magnetic field is greater than in the case (ii). As a result the simulation time for the required accuracy is longer. Moreover, within the turbulent volume, at a large distance from the centre the function $daw$ grows slower resulting in less efficient acceleration. For these reasons in the present simulations we consider solutions determined with the condition (ii) satisfied. We take the following values of the model parameters: $\alpha = 1.0 \cdot 10^{-9}$, $\lambda = \frac{\beta}{\alpha}$, where $\beta = 1.0 \cdot 10^{-10}$,

$\eta = 1.0 \cdot 10^{-6}$, $k = 0.15$, $\rho = M_p \cdot 10^{16}$ ($M_p$ proton mass), $\xi = 0$, $Z(0) = 0$, $Z'(0) = 7 \cdot 10^{-4}$. Values of these parameters were derived from fitting the model magnetic, electric and velocity field to the mentioned solar flare conditions, with the plasma density equal to $10^{16}$ m$^{-3}$.

Let us note that the simple analytic form of the considered solution limits the range of physically acceptable parameters to provide the possible boundary values of $\vec{V}$, $\vec{B}$, $\vec{E}$. In the present simulations we choose such boundary values for the solution at the edge of our considered volume to provide physical parameters near the reconnection layer that are close to the ones estimated for the solar flares. In the vicinity of the reconnection area, just outside of the reconnecting current layer, the magnetic field induction is assumed to be $B = 1.68 \cdot 10^{-3}$ T and the respective gyroradius (gyroperiod) for a 1 MeV proton is $r_g = 87$ m ($T_g = 4 \cdot 10^{-5}$ s), and $r_g = 3.4$ km ($T_g = 8.1 \cdot 10^{-5}$ s) for a 1 GeV proton. The assumed linear dimensions of the full considered reconnection region are $\Delta x = 2 \cdot 10^4$ km, $\Delta y = 2 \cdot 10^5$ km and $\Delta z = 1.5 \cdot 10^5$ km. The size of the volume of the perturbed magnetic field is in the centre $\Delta x = 2 \cdot 10^3$ km, $\Delta y = 6 \cdot 10^3$ km and $\Delta z = 2 \cdot 10^3$ km. One should note that the selected particular conditions are not essential for the presented considerations.

## 2.2 Monte Carlo modelling procedure

In the simulations we used a Monte Carlo approach including a trajectory splitting technique to improve statistics at larger energies (cf. Ostrowski 1991). To derive particle spectra we recorded 'weights' of particles escaping from the simulation volume in a given energy range. For every escaping particle a randomly[*] chosen particle still active in the simulations was split into two identical particles, each with half the weight of the original particle. Then the trajectories of both particles were followed, but due to the applied random momentum scattering they evolve in different ways. The maximum simulation time $t_{max}$ ($t_{max}$ is the upper limit in Fig. 4) was chosen to be sufficiently large to be unreachable by high weight particles. Thus any further increasing of $t_{max}$ does not influence the resulting spectra in a visible way.

In the simulations, we inject test particles with initial energy $E_0 = 2$ MeV in the vicinity of the reconnection null point and we follow their trajectories by numerical integration of particle equations of motion. The integration is completed when a particle either crosses the boundary of the considered reconnection region ('escape boundary'), or the time limit $t_{max} = 100$ s is reached. Particles were scattered in a small region around the reconnection null point only. This region is shown in the two upper panels of Fig. 1 as black rectangles, and in expanded form in the lower panel. The trajectory computation times are much longer for low energy particles and this is the main reason why we start with initial proton energies substantially larger than the thermal energy; for the discussion of the injection problem of energetic solar flare particles one can consult the discussion in Miller et al. (1997). As the long integrations performed

---

[*] With probability of selecting a given particle being proportional to its weight.

here require high accuracy we use a variable step fourth-order Runge-Kutta integration with the parameters chosen in such a way that any further accuracy increase does not affect the simulated trajectories. In the simulation we use only 100 particles because the required high accuracy of integration leads to extensive integration times. Let us remember that with the applied trajectory splitting technique the number of particles forming the spectrum at different energies is the same.

We performed a number of numerical tests of the code applied in the simulations. We checked by hand the derivation of the resulting particle phase space co-ordinates in a few randomly chosen individual integration steps of the code algorithm. Then we derived particle trajectories within a few simple uniform magnetic fields oriented randomly with respect to the chosen reference frame. The results coincided within the numerical accuracy with the derived analytic trajectories. Finally, for the actual considered magnetic field structure in the reconnection volume we positively checked conservation of particle energy with the plasma velocity set equal to zero.

In the simulations particles gain energy mostly in the vicinity of the reconnection layer when drifting in the $\vec{V} \wedge \vec{B}$ electric fields. Away from this region, while moving across the magnetic field gradient, particles can gain and lose energy, but the mean energy change is small. Somov & Kosugi (1997) estimated the accelerated particle energy as a product of the magnetic field, the plasma velocity and the reconnection area length. The energy gains derived in our *unperturbed* reconnection model are in agreement with this estimate if we take the distance traversed by a particle within the reconnection area as the required length. The effect of particle escape from the reconnection volume has been discussed by Speiser (1965) for a highly simplified reconnection model. We confirm his results showing that a small vertical magnetic field component within the reconnection layer increases the particle escape substantially.

In the simulations we consider the particle scattering process only in a small volume containing the reconnection null point, where the magnetic energy is dissipated (see Fig. 1). The real reconnection regions are expected to show analogous structures, with the turbulence amplitude growing toward the centre, including null points of the magnetic field. This choice also resulted from the fact that the Craig et al. (1995) three dimensional model of the stationary reconnection is not too realistic at large distances from the null point, as, for example, it involves the inflow velocity growing without a limit when increasing distance from the centre. For the perturbed trajectories model we use a simple pitch-angle scattering approach (e.g. Ostrowski 1991) intended to model the particle scattering at MHD waves. In this case integration of the particle equations of motion is performed in the electromagnetic field defined by the unperturbed analytic model, but trajectory perturbations are introduced every constant time interval $\Delta t$, when the particle momentum vector is randomly scattered within a narrow cone along its original direction. The scattering is performed in the local *plasma* rest frame and it conserves particle energy in this frame. In the present simulations we consider the uniform momentum scattering within a cone with the half opening angle equal to 11°. The perturbation intensity is controlled by changing $\Delta t$ and it is characterized with $\aleph \equiv \kappa_\perp/\kappa_\parallel$, the

ratio of the cross-field diffusion coefficient to the diffusion coefficient along the magnetic field. The value of $\aleph$ was determined in auxiliary simulations performed in the uniform magnetic field with the value characteristic for a region close outside the reconnection current sheet (see section 2.3). One should also note that decrease of the magnetic field toward the reconnection site leads to increasing the effective turbulence amplitude (i.e. the value of $\aleph$; in the limit of $B = 0$ we have $\aleph = 1.0$), but in the present simulations the particle gyroradius is always larger than the reconnection layer thickness near the considered X-type null point.

As the mean scattering time $\Delta t$ is assumed to be constant within a given simulation run, particle trajectories are affected by perturbations with intensity depending on particle energy and the background magnetic field. For non-relativistic particles with constant angular velocities of their gyration movements, assuming constant $\Delta t$ is equivalent to introducing scattering acts at constant gyrophase steps. Thus the resulting value of $\aleph$ does not depend on energy, as expected for the flat wave power spectrum $F(k) \propto k^{-1}$. This slightly unrealistic wave spectrum allows, on the other hand, evaluation of the role of diffusive effects for the same scattering amplitude at all considered particle energies. A discussion of a more realistic Kolmogorov wave spectrum within the finite wave vector range will be presented in the next paper (in preparation). However, as such a wave spectrum carries more energy in long waves, the results are expected to show a transition from our low $\aleph$ results to the large $\aleph$ ones.

In attempting to compare our simplified scattering model with the real turbulence with an amplitude of waves resonant for a particle of a given energy, $\delta B_r$ ($\delta B_r^2/8\pi \approx F(k_r) \cdot k_r$, where $k_r = 2\pi/r_g$), one can refer to a qualitative discussion of energetic particle diffusion presented by Drury (1983). With his scaling $\kappa_\parallel \propto (\delta B_r/B)^{-2}$ and $\kappa_\perp \propto (\delta B_r/B)^2$, the amplitude for resonance waves can be evaluated as $\delta B_r/B \approx \aleph^{1/4}$.

### 2.3    Derivation of the $\aleph \equiv \kappa_\perp/\kappa_\parallel$ parameter

The respective values of $\aleph \equiv \kappa_\perp/\kappa_\parallel$ were derived in auxiliary simulations involving the spatially uniform background magnetic field with the induction of $1.5 \cdot 10^{-3}$ T and particles with energies equal to the initial energy $E_0 = 2$ MeV. Trajectories of a large number of particles were followed with the imposed scattering process involving the momentum angular scattering, uniform within a cone of half opening angle equal to 11° and with the cone axis directed along the original momentum vector. The only parameter varying between the simulations was the time interval between successive scattering events, $\Delta t$. The resulting diffusion coefficients were derived from growing particle dispersions along the background field ($\kappa_\parallel$) and along two orthogonal axes perpendicular to the background field ($\equiv$ along the 1- or 2-axis). The results of such computations are presented in Fig. 2. Presentation of two derived values of $\kappa_1/\kappa_\parallel$ and $\kappa_2/\kappa_\parallel$ allows one to evaluate the accuracy of these computations. The values used in the paper are fits to the asymptotic ($T \to \infty$) value of $\aleph = 0.5 (\kappa_1 + \kappa_2)/\kappa_\parallel$. For a sequence of scattering times $\Delta t = 10^{-6}$, $10^{-5}$, $10^{-4}$ and $10^{-3}$ we derived the respective values of $\aleph = 1.2 \cdot 10^{-2}$, $6 \cdot 10^{-3}$, $6 \cdot 10^{-5}$, and $6 \cdot 10^{-7}$. The re-
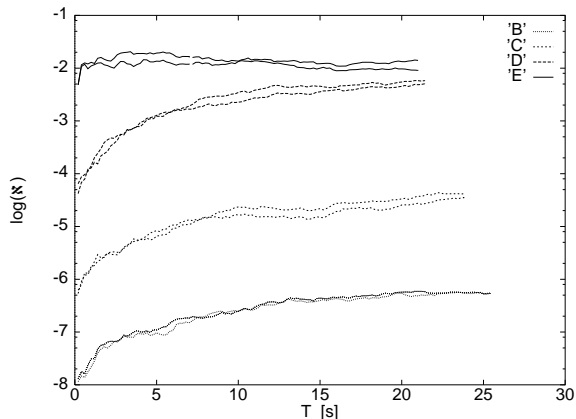
**Figure 2.** The diffusion parameter $\aleph \equiv \kappa_\perp/\kappa_|$ calculated during particle distribution evolution. $T$ is the simulation time. For given initial parameters one has two resulting values of $\aleph$ for $\kappa_\perp = \kappa_1$ and $\kappa_\perp = \kappa_2$, presented as separate lines.
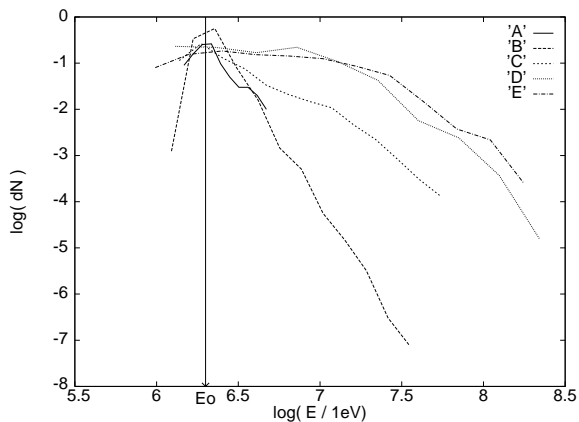


**Figure 3.** The resulting energy spectra for protons injected at $E_0 = 2$ MeV: Model A: $\aleph = 0$ (the unperturbed model), Model B: $\aleph = 6 \cdot 10^{-7}$, Model C: $\aleph = 6 \cdot 10^{-5}$, Model D: $\aleph = 6 \cdot 10^{-3}$, Model E: $\aleph = 1.2 \cdot 10^{-2}$. A vertical $E = E_0$ line is provided for a reference.

sults derived without applying any scattering are indicated by $\aleph = 0$.

## 3 SPECTRA OF ACCELERATED PARTICLES

In order to provide qualitative evaluations of turbulence effects in the volume of reconnecting magnetic field, but considering it only as a factor introducing random motion component to particle trajectories, we performed simulations of energetic proton spectra with a varying amount of turbulence ($\equiv$ scattering). As explained above, this approach assumes the existence of short wave magnetic field perturbations to be present in the limited volume – the black rectangle in Fig. 1 – near the central neutral point, but we do not consider the influence of the turbulence on the reconnection process. Thus it is a complementary approach to that using MHD modelling of the turbulent reconnection including wave perturbations from a narrow wave vector range, as discussed in section 1.
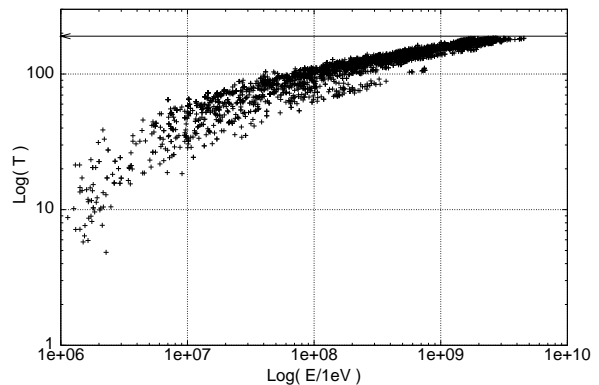


**Figure 4.** Acceleration times, $T$, versus the final particle energies, $E$, in the Model C (cf. Fig. 3). The simulation time cut-off at $t_{max} = 100$ s is indicated with a dashed line. Due to the applied trajectory splitting procedure the particles represented by points close to $T = t_{max}$ have very small weights and further increasing $t_{max}$ does not lead to modification of the spectra presented in Fig. 3.

We performed simulations of particle evolution starting at the same 'injection' energy $E_0 = 2$ MeV, avoiding consideration of the real injection process at much lower energies (cf. Miller et al. 1997). For each set of particles we derived the spectrum of particles escaping from the reconnection volume, as illustrated in Fig. 3. In the non-perturbed model ($\aleph = 0$, curve A) protons can increase their initial energy by approximately 70% . One should note that the injected energetic particles can gain as well as loose energy. Introducing trajectory perturbations results in substantial modification of the acceleration process (curves B, C, D, E in Fig. 3). The spectrum energy cut-off shifts to higher values and the spectrum becomes harder when the amount of scattering ('turbulence amplitude') is increased. In our simulations the resulting flat spectra extend up to 50 MeV for models with strong turbulence (Model D and E), and a steeper part of the spectrum is recorded at energies above 100 MeV. This behaviour results from the fact that the diffusive component introduced in to particle trajectories by the scattering enables some particles to stay in the reconnection region much longer and diffuse back close to the null point from outside. As illustrated, this can have a pronounced influence on the acceleration process by substantially increasing the particle mean energy gain and providing much larger energies of individual particles. There is a general trend for the acceleration efficiency to increase with the perturbation amplitude in the considered range of values for the $\aleph$ parameter.

Acceleration by the uniform electric field is characterized with the energy-independent rate of particle energy increase, leading to a linear relation between the particle acceleration time and its final energy. In contrast, a plot of correlation between the individual particle acceleration time ($\equiv$ the physical simulation time) and its final energy presented in Fig. 4 shows that the acceleration rate depends on energy, being preferentially defined by particle drifts in the '$V$ x $B$' electric fields. A large energy dispersion in a given time reflects variety of involved particle diffusive trajectories.

## 4    FINAL REMARKS

Consideration of energetic particle acceleration accompanying the magnetic field reconnection process requires knowledge of the electromagnetic field structure in the region of interest. Until now the available numerical models of such fields were oversimplified and fail to consistently include together the short and long MHD wave modes. Therefore, in the present simulations we apply an analytic model for a reconnecting field as the background, and the particle scattering process is imposed as the small amplitude uncorrelated angular momentum perturbations. A comparison of the acceleration process in such a model to the unperturbed model reveals the important result that inclusion of the turbulent field component into the reconnection volume can change the acceleration process in a *qualitative* way, enabling particles to reach much higher final energies and significantly increase their mean energy gain.

A serious limitation on the validity of our simplified modelling arises due to a non-self-consistent introduction of the MHD turbulent field. The trajectory perturbations in the turbulent medium are considered without taking into account the influence – in both directions – of these turbulent motions on the reconnection process itself. As mentioned in section 1, the presence of magnetic field turbulent structures increases mixing in the medium and is the source for anomalous resistivity leading to more effective reconnection as discussed recently by Lazarian & Vishniac 2000. Subsequently, it leads to more efficient particle acceleration (Matthaeus et al. 1984, Ambrosiano et al. 1988, Scholer & Jamitzky 1989, Veltri at al. 1998, Birn & Hesse 1994, Kliem et al. 1998, Schopper et al. 1999). As discussed in the present paper from a slightly different perspective it is expected to increase the cosmic ray acceleration efficiency, and influence the involved time scales and details of the resulting energy spectrum. However, for a given scattering conditions within the reconnection region the spectrum upper energy cut-off is limited by the 'global' perturbed structure of the reconnecting volume and not by the local conditions within the thin reconnection current sheet.

## REFERENCES

Ambrosiano J., Matthaeus W.H., Goldstein M.L., Plante D., 1988, JGR, 93, 14383
Atkinson, G., Creutzberg F., Gattinger R.L., 1989, JGR, 94, 5292
Birn J., Hesse M., 1994, JGR, 99, 14891
Craig I.J.D., Fabling R.B., Henton S.M., Rickard G.J., 1995, ApJ, 455, L197
Deeg H.-J., Borovsky J.E., Duric N., 1991, Phys. Fluids B, 3, 266
Drury L'O.C., 1983, Rep. Prog. Phys. 46, 973
Giacalone J., Jokipii J.R., 1994, ApJ, 430, L137
Goldstein M.L., Matthaeus H.W., Ambrosiano J.J., 1986, Geophys. Res. Lett., 13, 205
Kliem B., Schumacher J., Shklyar D. R., 1998, Adv. Space Res., Vol. 21, No. 4, pp.563-566,
Lazarian A., Vishniac E., 1999, Rev. Mex. A. A., in press (astro-ph/0002067),
Martin R.F., 1986, JGR, 91, 11985
Michałek G., Ostrowski M., 1996, Nonlinear Proc. Geophys., 3, 66
Michałek G., Ostrowski M., 1998, A&A, 337, 793
Miller J.A., Cargill P.J., Emslie A.G., Holman G.D., Dennis B.R., LaRosa T.N., Winglee R.M., Benka S.G., Tsuneta S., 1997, JGR, 102, 14631
Moses R.W., Fin J.M., Ling K.M., 1993, JGR 89, 4013.
Ostrowski, M., 1991, MNRAS, 249, 551
Sato T., Matsumoto H., Nagai K., 1982, JGR, 87, 6089
Schlickeiser R., Miller J.A., 1998, ApJ, 492, 352
Scholer M., Jamitzky F., 1987, JGR, 92, 12191
Scholer M., Jamitzky F., 1989, JGR, 94, 2459
Schopper R., Birk G.T., Lesch H., 1999, Physics of Plasmas (in press)
Somov B. V., 1994, *'Fundamentals of Cosmic Electrodynamics'*, Kluwer Academic Publishers, Dordrecht, Holland
Somov B. V., Kosugi T., 1997, ApJ, 485, 859.
Sonnerup B. U. Ö., 1971, JGR, 76, 8211
Speiser T. W., 1965, JGR, 70, 17
Stern D.P., JGR, 84, 63
Veltri P., Zimbardo G., Taktakishvili A.L., Zelenyi L.M., 1998, JGR, 103, 14987
Wagner J.S., Gray J.R., Kan J.R., Tajima T., Akassofu S.L., 1981, Planet Space Sci., 29, 391
Zelenyi L.M., Lominadze J.G., Taktakishvili A.L., 1990, JGR, 95, 3883